IET Renewable Power Generation

Research Article

IET Journals
The Institution of Engineering and Technology

Crowded plant height optimisation algorithm tuned maximum power point tracking for grid integrated solar power conditioning system

ISSN 1752-1416
Received on 15th April 2018
Revised 28th March 2019
Accepted on 3rd June 2019
E-First on 1st July 2019
doi: 10.1049/iet-rpg.2018.5053
www.ietdl.org

Nammalvar Pachaivannan[1] ✉, Ramkumar Subburam[2], Umadevi Ramkumar[3], Padmanathan Kasinathan[4]

[1]*Department of Electrical and Electronics Engineering, Krishnasamy College of Engineering & Technology, Cuddalore, India*
[2]*Department of Electrical and Electronics Engineering, New Horizon College of Engineering, Bengaluru, Karnataka, India*
[3]*Department of Electrical and Electronics Engineering, PSG Institute of Technology and Applied Research, Coimbatore, Tamilnadu, India*
[4]*Department of Electrical and Electronics Engineering, Agni College of Technology, Chennai, Tamilnadu, India*
✉ *E-mail: alvar1976@gmail.com*

Abstract: Solar energy is the base for both photovoltaic (PV) power generation and plant growth. Inspired by this biological phenomenon, a novel crowded plant height optimisation (CPHO) algorithm was developed for solar PV maximum power point tracking (MPPT). This CPHO-tuned MPPT algorithm was developed with the aim of obtaining the optimal duty cycle (*d*) for DC-DC boost converter for maximum solar power extraction from PV panels with the help of a proportional-integral controller. Crowded plants regulate the growth of their stem height in relation to neighbouring plants, also known as height convergence. Using this CPHO-algorithm, the stable height of the plant found in a numerical value is taken as the optimal height of the plant. This optimal numerical value was converted into (*d*) for the converter. Under dynamic weather conditions, the (*d*) was optimally adjusted by the proposed algorithm to regulate the DC output of the converter. On the utility side, *d–q* vector control-based voltage source inverter was used for PV power integration into the grid. The performance of the converter control strategy of the proposed CPHO algorithm was compared with perturb and observe algorithm-based MPPT control, which was analysed on MATLAB/Simulink platform.

1 Introduction

The preference for solar energy has reached a peak as it is the world's most popular renewable source for generating electricity. It is evident that around 18% of the people across the globe do not have electrification owing to lack of infrastructure such as power grids to supply electricity, a study states [1]. In the past decade, the Government of India has taken a lot of initiatives such as subsidies to promote solar power generation especially among people who live in remote areas. Furthermore, in order to meet the energy demands for the current scenario, large solar power projects only seem to be the best optimum solution. India has set an ambitious target of generating 175 GW of electric power from renewable energy resources by 2022 out of which 100 GW is planned exclusively from solar energy. Moreover, the cost of solar photovoltaic (PV) module got radically reduced [2, 3] by 26% over the years, 2012–2018.

In terms of the significance of maximum power tracking [4–6] in the PV system, the insolation variation of the sunlight throughout the day causes variation in the output power of the solar PV module. The irradiance value and the temperature of the PV module decide the output of PV proportionately. The above-mentioned effect deteriorates the efficiency of the PV module. Normally, a DC–DC converter is used to extract the maximum power from solar PV. The non-linear characteristic of a PV array is known and there occurs the best operating point [7] where the PV array produces the maximum power. To enhance the efficiency of the solar cell, it is important to concentrate on maximum power point tracking (MPPT) algorithm [8], which is used for harvesting solar energy.

It is no overstatement that the optimisation algorithm is critical for MPPT. Researchers are continuously attempting to find a robust algorithm for solar MPPT controller tuning [9, 10]. A great deal of these algorithms has been inspired by nature and biological systems. In the last decade, meta-heuristic (biology-based) algorithms [11] were proposed as a solution to optimisation problems. Meta-heuristic algorithms cover techniques that begin with the initial set of variables as 'population', which conclude by achieving the global minimum or maximum [12] of the fitness function.

The most recent bio-inspired metaheuristic algorithms [13] are seed-based plant propagation algorithm, lion optimisation algorithm, optic-inspired optimisation, raven roosting optimisation algorithm, vortex search algorithm, water wave optimisation, collective animal behaviour algorithm, bumblebees mating optimisation, artificial chemical reaction optimisation algorithm, bull optimisation algorithm and elephant herding optimisation [14]. Furthermore, plant-oriented algorithms, in particular [15], are flower pollination algorithm, invasive weed optimisation, paddy field algorithm, root mass optimisation algorithm, artificial plant optimisation algorithm, sapling growing up algorithm, photosynthetic algorithm, plant growth optimisation, root growth algorithm, strawberry algorithm as plant propagation algorithm, runner root algorithm, path planning algorithm and rooted tree optimisation. Even though a number of algorithms are available, the proposed crowded plant height optimisation (CPHO) algorithm smartly regulates the PV power with a DC–DC converter and produces the most extreme conceivable yield.

In this research work, the test system structures two power converters namely PV side converter and grid side converter. The DC–DC boost converter with the proposed CPHO algorithm-tuned MPPT control is used to reap the maximum power from the PV array. In general, DC–DC converters are controlled by well-known perturb and observe (P&O) tuned MPPT since it seems to be easy in terms of implementation. However, it is challenging to determine the best perturbation value. A smaller perturbation value reduces the algorithm tracking performance whereas high-perturbation value results in oscillation when determining maximum power point (MPP). Also, during the solar insolation variation, the P&O algorithm is prone to error and produces large changes in duty cycle variation. Indeed, even incremental conductance and hill climbing MPPT control methods also failed to serve under rapid insolation variation. Besides, P&O consumes more convergence time with fluctuations. The proposed CPHO algorithm enhances the determination of MPP, under rapidly varying atmospheric conditions, with higher accuracy than the

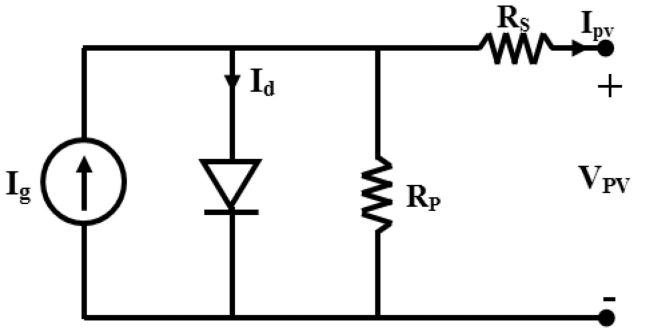

Fig. 1 *Equivalent circuit of a single diode PV cell*

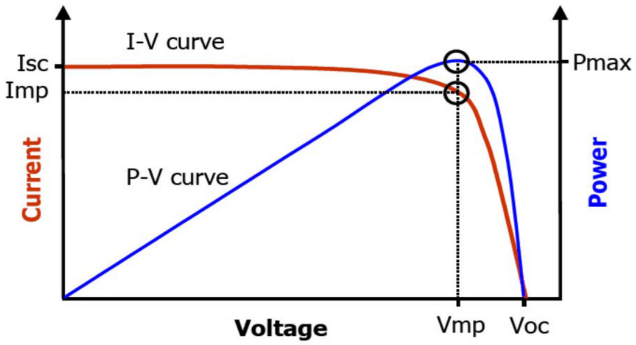

Fig. 2 *Output characteristics of PV array*

Table 1 Solar module specification – 'SunPower SPR-305-WHT'

Parameters	Specification
number of cells in series	$nCells = 96$
maximum power, W	$P_{mp} = 305.2$
maximum power voltage, V	$V_{mp} = 54.70$
maximum power current, A	$I_{mp} = 5.58$
open circuit voltage, V	$V_{oc} = 64.20$
series resistance of PV model, Ω	$R_s = 0.037998$
parallel resistance of PV model, Ω	$R_p = 993.51$

P&O method and is validated by the simulation results in this work. A DC–AC converter, known as voltage source inverter (VSI), is employed for PV power integration into grid and it works on the basis of *d–q* vector control [16, 17]. This *d–q* control acquires the data such as grid voltages, grid currents, PV voltage, and DC voltage and evaluates the data to generate gate control signals. This control technique enhances the stability of the system and ensures there is less oscillation in the AC grid system [18]. The behaviour of the *d–q* vector control is evaluated through transient simulation studies.

In this study, PV modelling and solar module specification chosen for a simulation study of a test system focus are discussed under Section 2. Section 3 proposes a novel optimised CPHO algorithm tuned control scheme for the DC–DC converter. Section 4 details the system configuration and converter control. The performance and comparative study of the proposed CPHO and P&O-based control strategies are given in Section 5. Finally, this paper concludes with a summary of the research work carried out.

2 Modelling of the PV system

A brief review of PV modelling, presented in this section, infers that PV characteristics can significantly influence the design and operation of power converter and control system. The circuit of a single diode is the model generally utilised as it seems to be a reasonably-good compromise between simplicity and accuracy. Fig. 1 demonstrates the equivalent of a single diode circuit of the PV cell. The circuit consists of a current source, a diode in parallel with the current source, the series resistance, and the parallel resistance.

The basic equation that describes the *I–V* characteristics of the PV model [19] is given by the following equation:

$$I_{pv}(V_{pv}) = I_g - I_d - \left(\frac{V_{pv} + R_s I_{pv}}{R_p}\right), \quad (1)$$

$$I_d = I_0\left[e^{q(V_{pv} + R_s I_{pv})/KT} - 1\right], \quad (2)$$

where $I_{pv}$is the cell current (A), I_g is the generated current (A), I_d is the diode current (A), I_o is the diode saturation current, q is the charge of electron = 1.6×10^{-19} coul, K is the Boltzmann constant (J/K), T is the cell temperature (K), R_s and R_p are PV cell series and shunt resistance (ohms), and V_{pv} is the cell output voltage (V).

The quality of a cell can be determined if open circuit voltage, short circuit current, the voltage at MPP, and current at MPP are known and once it is known; it is easy to obtain the operating power point. The first step is to plot voltage versus power graph of the cell. Power was calculated by multiplying voltage across the cell with the corresponding current in the cell. In the plot, MPP is located and the corresponding voltage is noted down. The second step is to locate the current corresponding to the voltage at MPP from the *I–V* characteristics of the cell. This current is called the 'current at MPP'. The point at which I_{mp} and V_{mp} meet is the exact MPP, which is shown in Fig. 2. This is the point where maximum power is available in the PV cell. If the 'load line' crosses this point precisely, then the maximum power can be transferred to this load. Table 1 shows the specification of the solar module chosen for the simulation studies.

3 Proposed CPHO algorithm

3.1 Biological inspiration

Various algorithms are available in the market to perform MPPT. For the high-efficient performance of MPPT system, the time taken to reach the required operating level is critical. The ability of the MPPT algorithm can be understood based on the speedy occurrence of PV power MPPT tracking operation convergence and how it matches with the reference tracking system. The proposed CPHO algorithm is a novel and bio-inspired meta-heuristic method for global optimisation and is perceived by the natural behaviour of crowded plant growth. The crowded plants regulate the growth of their stem height to maintain similar height level of neighbouring plants. Here the photosynthetic process of the plant that competes for light is considered. Even though being tall is more advantageous for sunlight competition among the plants, height convergence observed among the crowded plant growth remains the base for proposing this algorithm. Based on sunlight competition that occurs during the survival of plants, a new CPHO algorithm is introduced in MPPT control via the current research work to harvest more power from solar PV. This concept was observed over a period of two years from an agricultural field study of the growth of eucalyptus tree from plant position to tree position. Then this CPHO algorithm was developed and implementation process was started on a single stem plant. This algorithm can also be extended using other varieties of plants. Before starting this algorithm research, the following assumptions were made considering a single stem plant and the study was conducted.

i. All the selected seeds are the best seeds and belong to the same variety.
ii. All the plants are transplanted on the same day.
iii. The transplanted area is considered as flat and equal surface.
iv. The manure, water supply, and fertiliser are applied to the plants in equal quantities.
v. The plants which are on the outer side row and column of land are not considered for evaluation.

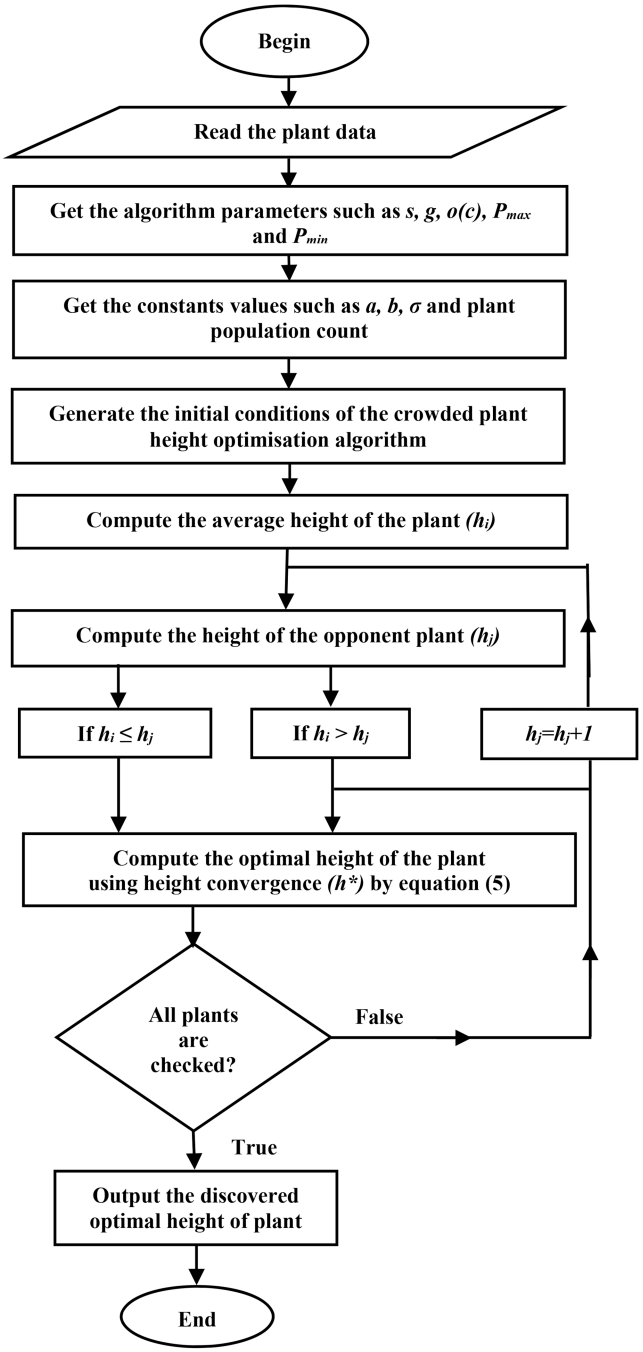

Fig. 3 *Flowchart for CPHO algorithm*

3.2 Theory of CPHO algorithm

Eucalyptus seeds were sown in the land with distributed space. After few weeks, these plants were transplanted to fields with recommended equidistance spacing in (row column) matrix format. The observation period over the plant was from the sixth month to 24th month. Now due to plant growth, the space between the plants become less and it becomes crowded. Sunlight is the resource for the photosynthetic process which is vital for plant growth and reproduction. The competition for sunlight starts among the neighbouring plants for survival and growth. In the crowd, short plants increased the rate of stem elongation to get solar irradiance while at the same time; plants which were comparatively taller reduced the rate of stem elongation to get reduced solar irradiance. Finally, the crowded plants converged to similar height [20].

Using the simulation model proposed by the authors of [20, 21], let us also consider the following additional factors:

s function of stem length
g function of the mean height of the opponent plant
h_i mean height or target plant height
h_j neighbouring plant height
h^* convergence height
σ proportional variation in mean plant height
$o(c)$ probability of horizontal overlap leaves
$P_{\max}$ photosynthetic rate per unit leaf mass of unshaded leaves
$P_{\min}$ photosynthetic rate per unit leaf mass of shaded leaves
$h_i(1\pm\sigma)$ leaves are distributed randomly on stems
$g(h_i, h_j)$ expected rate of photosynthesis

The height of the plant alone is not considered for optimal plant selection. Here the researchers considered some additional criteria to find the optimal height. The mean height of the plant is taken as h_i and competitor plant height is taken as h_j. When the average plant height is taller than the neighbouring plant ($h_i > h_j$), (3) is used to find the expected rate of plant growth based on photosynthesis

$$g(h_i, h_j) = P_{\max} - \left[\frac{\left[h_j(1+\sigma) - h_i(1-\sigma)\right]^2}{4h_i h_j \sigma^2}\right] \times \frac{O(c)}{2} \times (P_{\max} - P_{\min}). \tag{3}$$

Similarly, when the average plant height is shorter than the neighbouring plant ($h_i < h_j$), (4) is used to find the expected rate of plant growth based on photosynthesis

$$g(h_i, h_j) = P_{\min} + \left[\frac{\left[h_i(1+\sigma) - h_j(1-\sigma)\right]^2}{4h_i h_j \sigma}\right] \times \left(1 - \frac{o(c)}{2}\right) \times (P_{\max} - P_{\min}). \tag{4}$$

Next, the height convergence of the crowded plant was calculated and the optimal numerical value was found using the following equation:

$$h^* = \frac{(a/b) \times o(c) \times (1 - (P_{\min}/P_{\max}))}{2\sigma + (1-\sigma) \times o(c) \times (1 - (P_{\min}/P_{\max}))}. \tag{5}$$

The numerical values of 'a' and 'b' were 0.73 and 0.0031, respectively, obtained from control plants in the simulation study because the leaves were subjected to sunny and shady environments as proposed by Givnish model. σ is 0.48 and $o(c)$ is regarded as one.

The flowchart for the CPHO algorithm is shown in Fig. 3 and was developed by utilising the above three equations.

4 System configuration and operation

4.1 PV system configuration

The layout of the proposed work is shown in Fig. 4 and the system configuration chosen for the simulation study is given in Table 2. The PV side DC–DC boost converter extracted the solar power using the proposed CPHO algorithm-tuned MPPT system whereas the utility side VSI employed d–q vector control.

4.2 Operating modes

The prime objective of the proposed scheme is to harvest the maximum amount of solar energy from the PV module that enhances the performance with the help of optimal control strategy. The effectiveness of the proposed AC network is categorised into three separate working modes.

Mode I: In the absence of AC local load, the entire PV power generated is integrated into the AC utility grid.
Mode II: When the PV power produced is surplus than the required power of local AC loads, the excess energy from solar PV is exported to the utility grid.

Mode III: Under the sunset condition, the irradiation of solar falling over PV module is not enough to meet the local AC load demand. During this condition, the system receives the demanded power from the utility grid.

4.3 Proposed CPHO algorithm tuned proportional–integral (PI) control

In the proposed approach, the parameters considered were voltage equated to the height of the plant, rate of plant growth equated to current and the photosynthesis process equated to irradiation and temperature.

These calculated parameters were fed as input to the CPHO algorithm to locate the MPP. At this juncture, the voltage from the PV array was compared with the reference voltage obtained from the CPHO algorithm. Meanwhile, the PV array was forced to generate maximum power using the CPHO algorithm and the optimal duty cycle (d) of the DC–DC converter [22] was controlled by the PI controller through the calculation of error between the reference voltage and the actual PV voltage.

To keep up the DC voltage constant for PV side and load variations, a PI controller was designed and implemented to reduce the variation at the output of the chopper. The PI controller, along with the novel CPHO algorithm, was considered here. The PI controller is common in process control or regulating systems and remains the ideal integral compensation. The gains of (K_p) and (K_i) in the proposed controller were found individually for each mode of operation and three sets of values were obtained using *a priori* test and to get the optimal duty cycle (d) tuned through the CPHO algorithm. In the current work, the performance was evaluated through three case studies and the process is a continuous one since the final best gain values shown in Table 3 of (K_p) and (K_i), were used with a presumption that it will allow the CPHO-PI for assuring at the desired performance.

Fig. 5 shows the simulation result of the duty cycle (d) under step-up irradiation change and presents the effectiveness of the CPHO-tuned PI controller. The zoomed view shows that the fluctuations were almost eliminated in the proposed controller. From the simulation results, it can be inferred that the response of the proposed CPHO-PI controller is much faster than that of the P&O tuned PI controller in a transitional state and the oscillations got diminished in the steady state.

A non-linear time domain analysis comparison was performed using simulation with a conventional P&O-PI MPPT controller and a CPHO-PI MPPT controller. An update frequency of 5 kHz and stable perturbation step size of 0.01 s were selected depending on the variation between the tracking speed and the fluctuations in the steady state for the CPHO-PI controller. The comparisons of the PV array power outputs of both P&O-PI and CPHO-PI controllers are shown in Fig. 6. From the figure, it is proved that based on the irradiation levels, the projected CPHO-PI controller is much fast in tracking than the existing P&O-PI controller. Particularly, the tracking time of the projected CPHO-PI controller was 0.04 s, whereas, in the case of the P&O-PI controller, it was 0.1 s with the first level of irradiation compared to the reference tracking line.

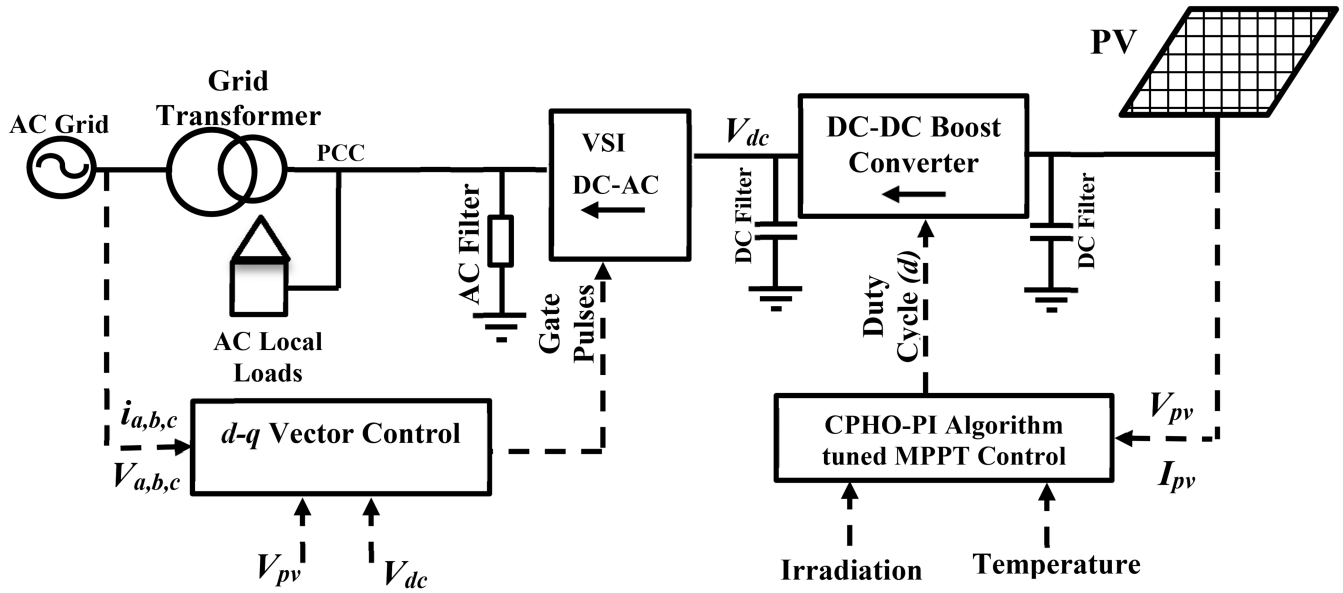

Fig. 4 *Complete layout diagram of the proposed PV power conditioning system*

Table 2 Specification of the system configuration parameters chosen for the simulation study

System specification	Parameter	Rating
AC grid	line voltage/frequency	120 kV, 50 Hz
VSI	rating	100 kVA
grid transformer	voltage rating	25 kV/120 kV
step up transformer	voltage rating	0.5 kV/25 kV
DC–DC converter	voltage/switching frequency	500 V/5 kHz
PV system	PV model parameters	refer Table 1
variable local load	unbalanced load	100 kVA, lagging

Table 3 Optimised PI parameters of controller gain

PI parameters	Proportional gain, K_p	Integral gain, K_d
CPHO	0.39	0.357
P&O	0.079	0.156

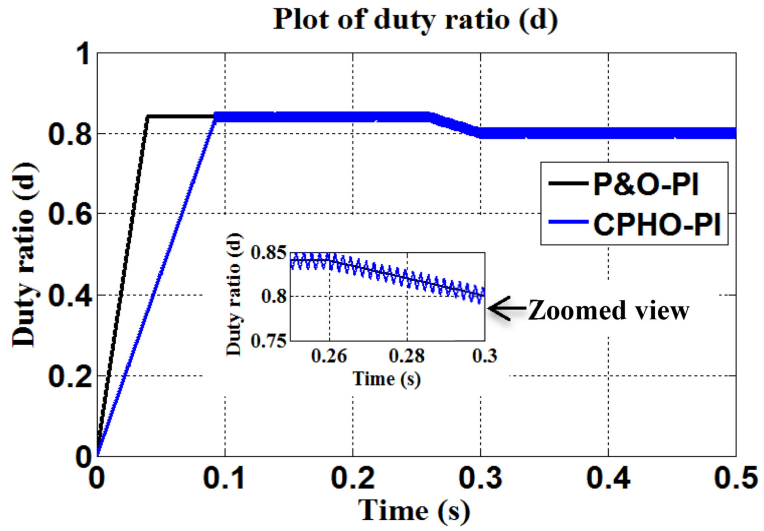

Fig. 5 *Duty ratio (d) under step-up irradiation change*

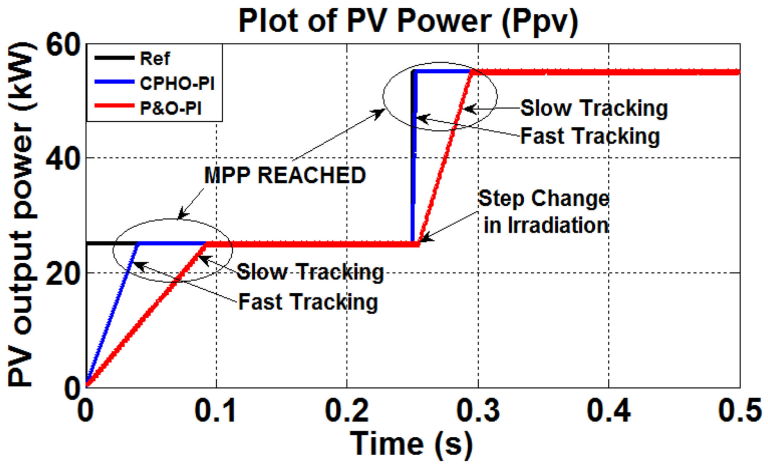

Fig. 6 *PV power tracking response characteristics*

4.4 VSI control method

In the traditional *d–q* vector control method, there is a nested loop topology as shown in Fig. 7 which includes an outer slow voltage loop and an inner fast current loop that produce *d*-axis and *q*-axis current references (i^*_d & i^*_q) [23, 24]. The purpose of the inner current controller is to diminish the two current errors such as the *d*-axis current error that may exist between the *d*-axis current reference i^*_d and the actual *d*-axis current i_d component; while the *q*-axis current error may exist between the *q*-axis current reference i^*_q and the actual *q*-axis current i_q component. The outer voltage controller has a DC voltage (V_{dc}) control and AC grid voltages. The DC voltage control can modify the *d*-axis current reference i^*_d on the basis of the difference between the actual and the reference capacitor voltages. However, AC voltage control modifies the *q*-axis current reference i^*_q depending on the difference between the actual and the reference AC grid voltages.

The objective function of the proposed CPHO algorithm is defined by the following equations:

$$\text{Minimise}: |V_{\text{bus}} = V^*_{\text{bus}}|, \tag{6}$$

$$\text{Subject to}: |V_{\text{bus}} = V^*_{\text{bus}}|, \quad \sqrt{\frac{V_{q1}^2 + V_{d1}^2}{3}} \le \frac{V_{\text{dc}}}{2\sqrt{2}}. \tag{7}$$

The converter output voltages V_{d1} and V_{q1}, depend on *d*-axis and *q*-axis reference voltages of V^*_{d1} and V^*_{q1}, and these are linearly proportional to each other. These voltages include *d* and *q* voltages V'_d and V'_q from the current controllers and in addition, the compensation relations are given in the following equations:

$$V^*_{d1} = -V'_d + \omega_s L i'_q + V_d, \tag{8}$$

$$V^*_{q1} = -V'_q - \omega_s L i'_d. \tag{9}$$

In this vector control technique, the voltage control signals V'_d and V'_q from the outer controller were utilised to regulate the current control signals i_d and i_q, respectively. The three-phase sinusoidal voltage references such as V^*_{a1}, V^*_{b1}, and V^*_{c1} were generated from two voltage references V^*_{d1} and V^*_{q1} to control the pulse-width modulation-based VSI. In order to make use of conventional PI control logic, the traditional *d–q* vector control method was used for both simplicity and enhancement in the system efficiency and performance.

In general, the traditional *d–q* vector control has four PI controllers of which two are located at the inner current loop while the remaining are positioned at the outer voltage loop. In the current study, the gain of the PI controllers at the outer voltage loop (AC voltage control and DC voltage control) is kept constant. The values of the proportional (K_p) and integral (K_i) controller gains of outer voltage loop controllers are shown in Table 4. Table 5 details the upper and lower limits for the optimal tuning of the PI controller gain at the inner current loop.

5 Case studies and simulation results

With the purpose of observing dominance and eminence of the proposed control scheme, a MATLAB/Simulink model was developed. The modelled test system with the proposed optimum CPHO-PI tuned MPPT control, along with standard *d–q* vector control for VSI was simulated independently for three case study

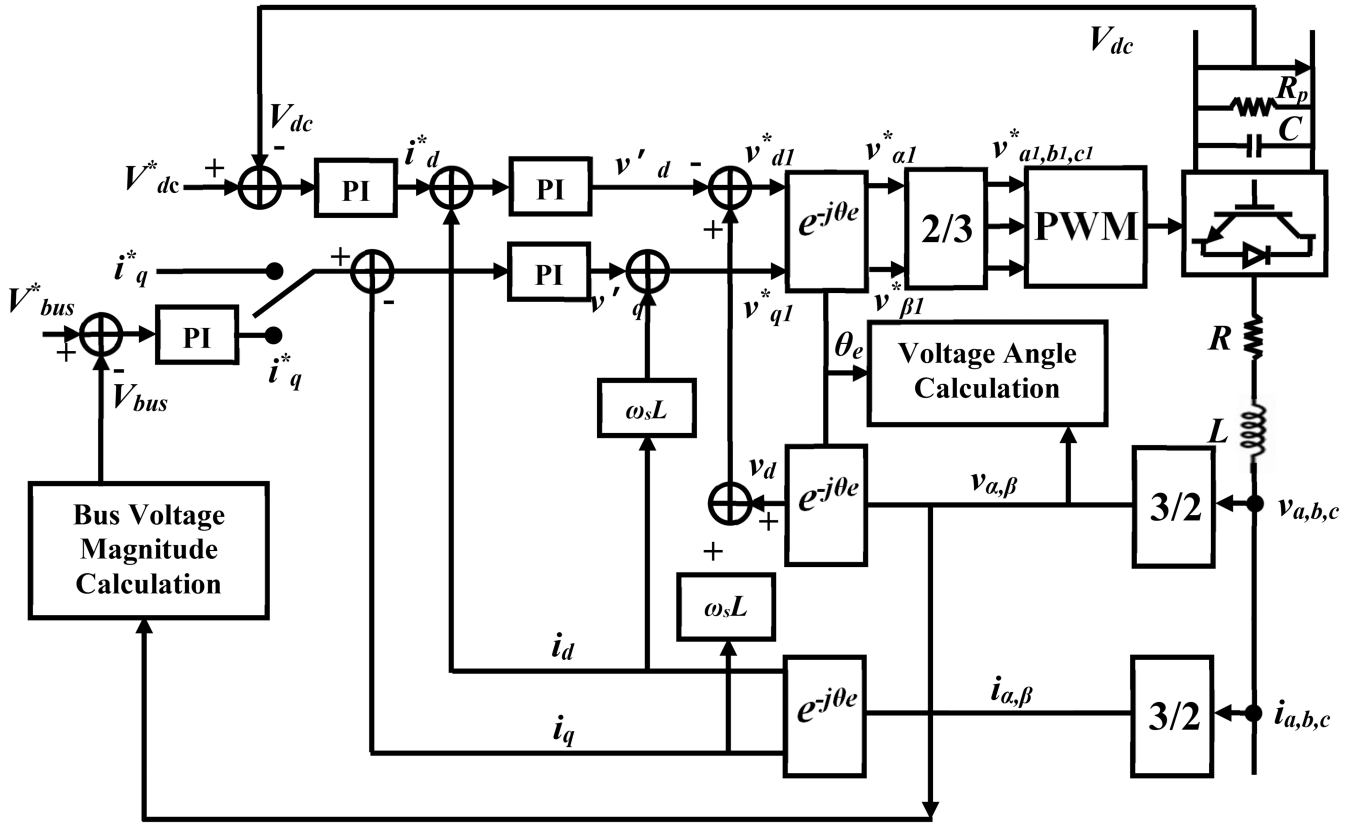

Fig. 7 *d–q vector control scheme for VSI*

Table 4 Controller gains for outer voltage loop

Parameters	Proportional gain, K_p	Integral gain, K_i
AC voltage regulation	0.45	2416
DC voltage regulation	0.098	0.145

Table 5 Range of PI controller gains for optimal tuning – current loop

Parameters	Proportional gain, K_p		Integral gain, K_i	
	Min	Max	Min	Max
d-axis	0.624	0.946	158	238
q-axis	0.614	0.926	152	236

modes. The implications inferred from the simulation studies were used to evaluate the performance in terms of maximising the power extraction from the PV panel, controlling the DC voltage and delivering the utmost renewable energy to the AC grid. During the time domain analyses of all the cases, the effect of solar insolation variation was taken into account at a constant temperature of 25°C. Initially, the solar insolation was at 1000 W/m^2 for 1 s which then varied randomly between 800 and 1000 W/m^2 for every second. The complete simulation was carried out over a 'simulation running time' of 10 s and the mean value of solar insolation falling on the PV panel was calculated as 890 W/m^2. The following section details the simulation case studies. In all the cases, the superiority of the proposed CPHO-PI tuned control scheme was compared against the traditional P&O-PI control schemes.

5.1 Case 1

In this test case, the PV power was integrated with the AC grid through the DC–DC converter and VSI. Furthermore, in this case, the entire power generated by PV was exported to the grid on the basis of the assumption that there is no live local AC load.

During the analysis, the PV side DC–DC converter was forced to operate in MPPT mode to harvest the maximum power from the solar panel whereas the VSI was operated to control the AC voltage into the grid. Figs. 8*a–c* show the solar insolation level, proportional PV terminal voltage, and regulated DC voltage for different solar insolation levels. Similarly, the DC power extracted from the PV panel with respect to the effect of sunlight intensity variation and the power exported to the AC grid was evaluated and the corresponding simulation responses are depicted in Figs. 9*a–c*. It can be concluded that the DC–DC converter, with the proposed CPHO-PI tuned MPPT control strategy, was able to smoothly regulate the DC voltage and VSI with *d–q* vector control was able to regulate the AC voltage during solar insolation variation.

5.2 Case 2

A fixed live local AC load of 50 kW at point of common coupling (PCC) was considered for the analysis. The remaining surplus PV power was exported to the utility grid. During the simulation, the PV was operated in MPPT mode and the DC voltage was regulated. The effect of solar insolation variation was considered in the simulation and is shown in Fig. 10*a*. The PV array MPP voltage at the terminal and the boosted DC voltage are shown in Figs. 10*b* and *c* for different solar insolation levels. The PV power extracted from panels, the fixed capacity of local AC load power and the power exported to the AC grid are illustrated in Figs. 11*a–d*. It is inferred that the VSI, with proposed CPHO MPPT control along with *d–q* vector control, efficiently controlled the AC voltage

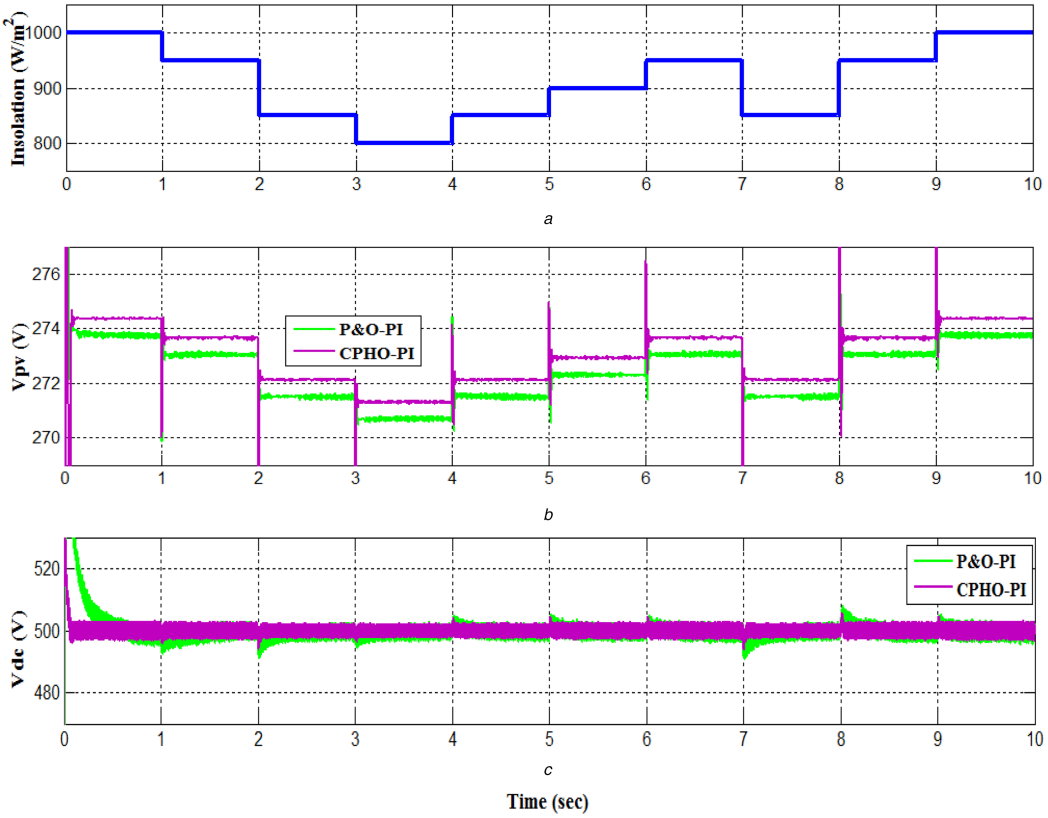

Fig. 8 *Compared MPPT system behaviour during PV generation variation in grid connected mode at a constant temperature of 25° C (case 1)*
(a) Solar insolation variation (W/m^2), ***(b)*** PV array voltage (volts), ***(c)*** Boosted DC voltage at VSI (volts)

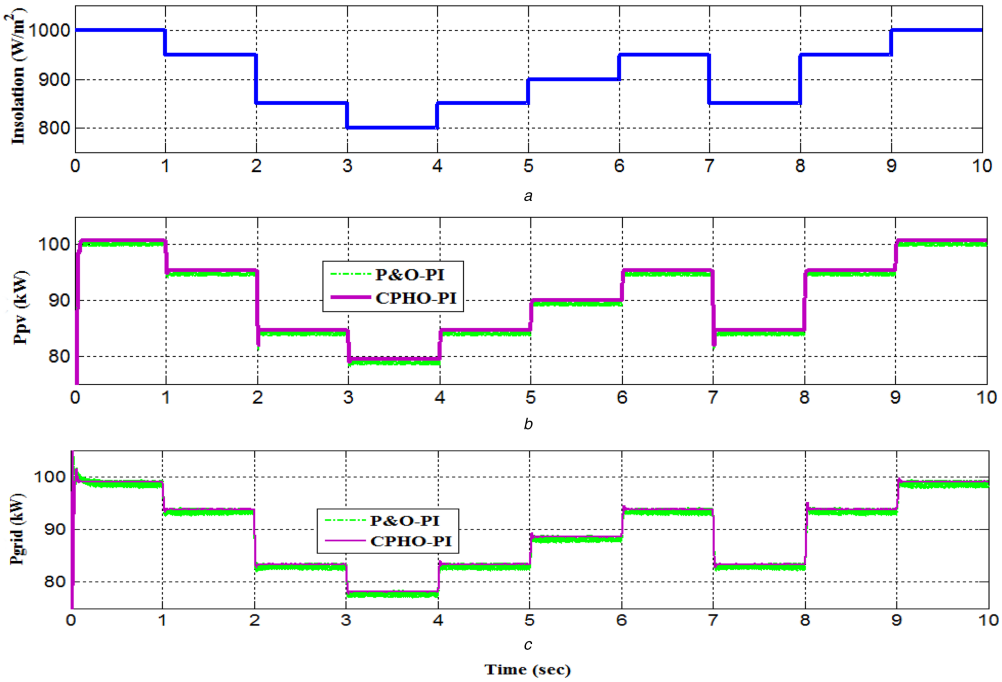

Fig. 9 *Compared MPPT system behaviour during PV generation variation in grid connected mode at a constant temperature of 25° C (case 1)*
(a) Solar insolation variation (W/m^2), ***(b)*** PV power generation (kW), ***(c)*** Total power exported to grid (kW)

than the conventional P&O-based MPPT control during solar insolation variation.

5.3 Case 3

In this case study, the scenario where the load demand is higher than the PV generation during sunset. In this situation, to provide reliable operation of variable local AC loads at PCC, the system imported the power, additionally required, from the utility grid. During the simulation study, the PV was always operated in MPPT mode and the VSI regulated the AC voltage. Similar to earlier case studies, the effects of solar insolation variation and load variation were considered for justification. Solar insolation variations, PV array voltage and DC voltage at the front end of VSI are shown in Figs. 12*a–c*. Variable local AC load power, generated PV power and the exported/imported power to the AC grid are illustrated in Figs. 13*b–d*. It is observed that the DC–DC converter, with the proposed controller, was able to regulate the DC voltage even under low solar insolation than the familiar P&O-based MPPT

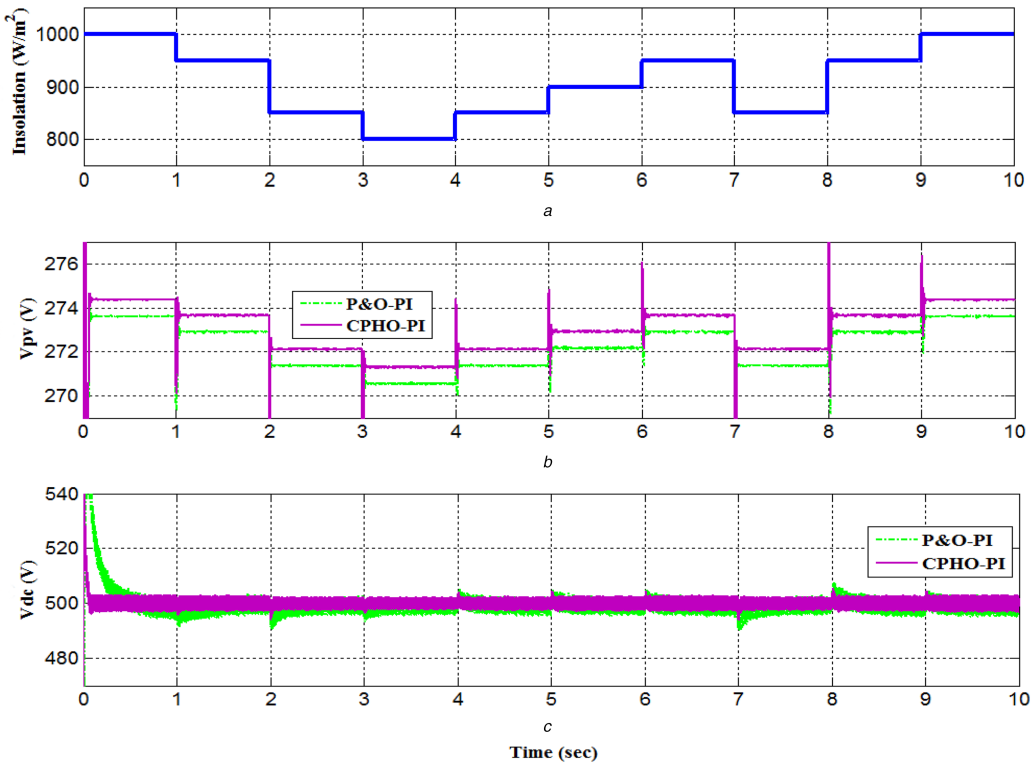

Fig. 10 *Compared MPPT system behaviour during PV generation variation in grid connected mode with fixed 50 kW local AC load at a constant temperature of 25°C (case 2)*

(a) Solar insolation variation (W/m^2), ***(b)*** PV array voltage (volts), ***(c)*** Boosted DC voltage at VSI (volts)

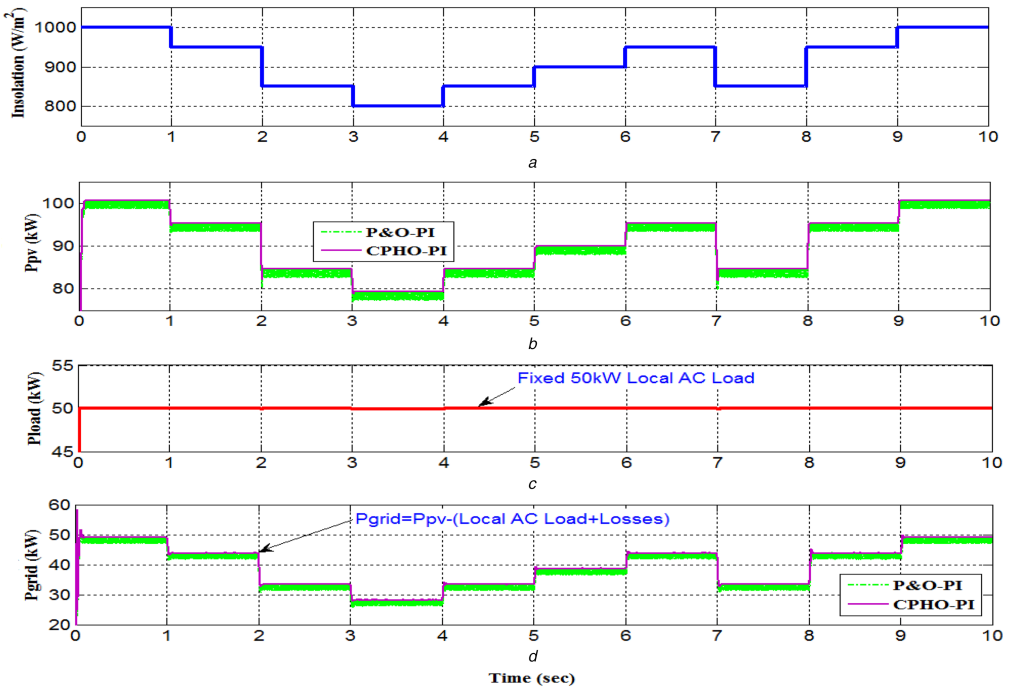

Fig. 11 *Compared MPPT system behaviour during PV generation variation in grid connected mode with fixed 50 kW local AC load at a constant temperature of 25°C (case 2)*

(a) Solar insolation variation (W/m^2), ***(b)*** PV power generation (kW), ***(c)*** Total power consumed by local AC load (kW), ***(d)*** Total power exported to grid (kW)

control, and the AC terminal voltage of VSI was also regulated by *d–q* vector control under different loading conditions.

5.4 Results inference

The system responses in terms of rise time, peak time, overshoot and settling time for both controllers were premeditated and presented in Table 6. From the tabulated values, it can be inferred that the proposed controller is optimum in all the conditions such as the steady-state analysis, line regulation, and load regulation. Next, the power conversion efficiency of the P&O control method and the proposed optimal CPHO control were compared for three case studies. From Table 7, it is evident that the proposed control scheme exhibited better performance than the existing control scheme with the improvement of a minimum of 0.29–0.89%. Under time varying solar insolation and load fluctuations, the voltage appeared across the PV panel may be higher or lower than the DC link voltage. The proposed algorithm-tuned DC–DC converter regulated the uncontrolled DC source from PV power and extracted the non-conventional energy efficiently. The VSI also

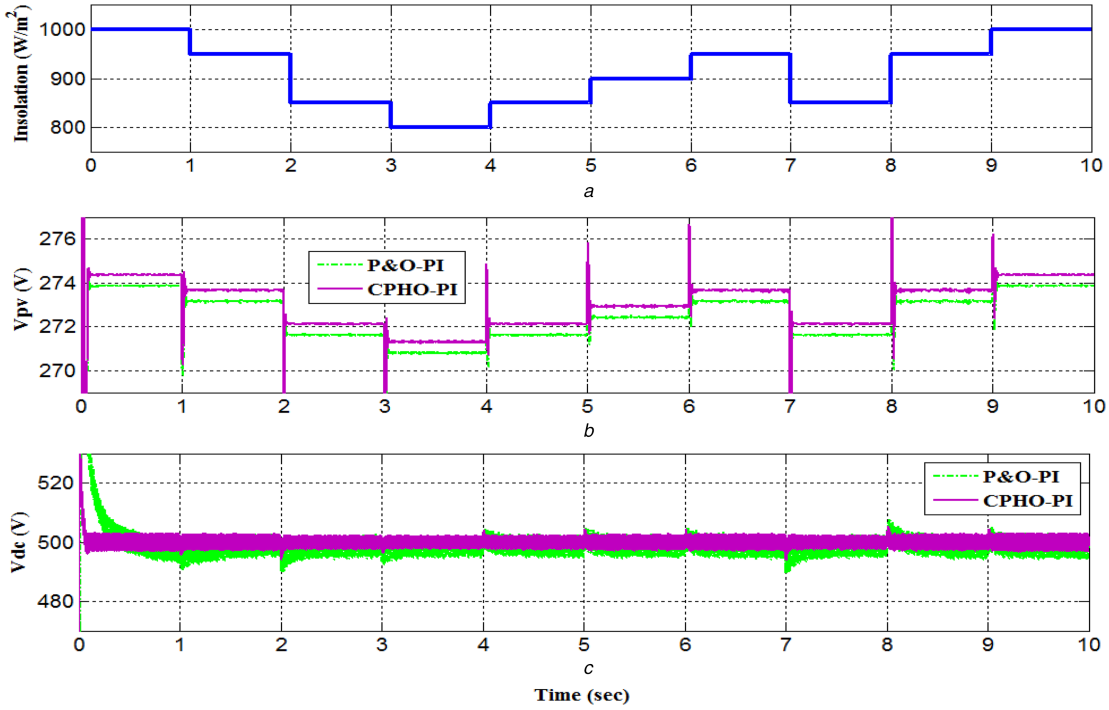

Fig. 12 *Compared MPPT system behaviour during PV generation variation in grid connected mode with variable local AC load at a constant temperature of 25°C (case 3)*

(a) Solar insolation variation (W/m^2), ***(b)*** PV array voltage (volts), ***(c)*** Boosted DC voltage at VSI (V)

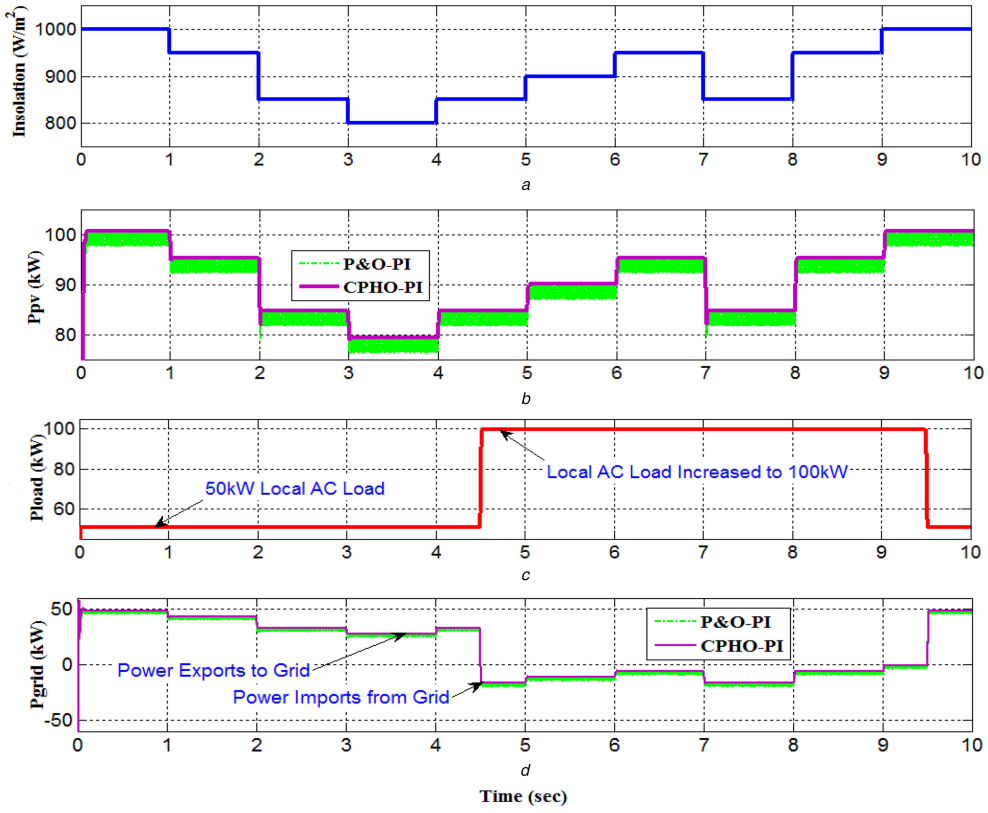

Fig. 13 *Compared MPPT system behaviour during PV generation variation in grid connected mode with variable local AC load at constant temperature of 25°C (case 3)*

(a) Solar insolation variation (W/m^2), ***(b)*** PV power generation (kW), ***(c)*** Total power consumed by variable local AC load (kW), ***(d)*** Total power exported to grid and imported from grid (kW)

exhibited better performance and robust operation. Furthermore, Table 7 shows that the proposed control scheme not only possess good stability and efficiency, but it also exhibits solid performance against time-varying solar insolation and different loading conditions.

6 Conclusion

An effective solar PV power conditioning system was developed using the proposed CPHO-PI controller for achieving an optimal duty cycle of a DC–DC converter system. The effectiveness of the controller was fortified by comparing the simulation results.

Table 6 Comparative performance evaluation analyses of P&O-MPPT versus CPHO-MPPT for DC to DC boost converter output voltage (V_{dc}) of the PV system using MATLAB

Case study	Controller	Steady state analysis			
		Rise time, s	Peak time, s	Over shoot, %	Settling time, se
case 1	P&O-PI	0.0096	0.013	12.91	0.065
	CPHO-PI	0.0039	0.006	4.89	0.030
case 2	P&O-PI	0.0098	0.011	11.12	0.055
	CPHO-PI	0.0040	0.008	3.52	0.040
case 3	P&O-PI	0.0099	0.010	11.02	0.050
	CPHO-PI	0.0041	0.006	3.50	0.030

Case study	Line regulation				Load regulation				DC voltage ripples, %
	PV array voltage increase by 20%		PV array voltage decrease by 20%		Load increase by 50%		Load decrease by 50%		
	Over shoot, %	Settling time, s	Under shoot, %	Settling time, s	Under shoot, %	Settling time, s	Over shoot, %	Settling time, s	
case 1	2.58	0.013	1.80	0.012	2.62	0.014	2.70	0.079	0.79
	0.97	0.006	0.68	0.005	1.56	0.005	1.25	0.006	0.63
case 2	2.22	0.011	1.55	0.010	2.30	0.012	2.73	0.080	0.72
	0.70	0.008	0.49	0.007	1.10	0.007	1.02	0.006	0.61
case 3	2.20	0.010	1.54	0.010	2.22	0.011	2.70	0.079	0.72
	0.70	0.006	0.48	0.005	1.00	0.006	1.22	0.005	0.61

Table 7 Comparison of power conversion efficiency of existing and proposed control strategy for various cases

Technique	Case 1		Case 2		Case 3	
	P&O-PI	CPHO-PI	P&O-PI	CPHO-PI	P&O-PI	CPHO-PI
solar average insolation for 10 s, W/m^2	890	890	890	890	890	890
average extracted power from PV panel, kW	90.87	91.16	90.26	91.01	90.02	90.72
average exported power to gird, kW	89.45	90.13	89.32	90.02	88.92	89.49
DC–DC converter power conversion efficiency, %	99.14	99.46	98.32	99.03	98.45	99.00
VSI power conversion efficiency, %	97.38	98.13	97.14	97.98	97.22	98.11

Furthermore, it can be understood from the results that the tracking time response of the proposed controller is superior to the existing familiar P&O-PI-based MPP tracking controllers in all aspects, even under non-linear and time-varying solar insolation. The maintenance of steady DC voltage, before applying to VSI, was ascertained by the proposed algorithm. The VSI is also identified as the objective of the integration of solar power into the grid by *d–q* vector control. The control scheme was perceived with two distinct operating modes, i.e. exporting power to the AC grid and importing power from the AC grid. The simulation studies executed in MATLAB Simulink platform inferred that the proposed CPHO algorithm performed competently in varying solar insolation. Finally, the proposed control scheme possesses superior system stability and power conversion efficiency over the well-known P&O algorithms.

7 References

[1] 'Solar rooftop-grid connected', Ministry of New and Renewable Energy (MNRE), Government of India. Available at http://www.mnre.gov.in/schemes/decentralized-systems/solar-rooftop-grid-connected/, accessed 02 February 2017

[2] Kasinathan, P., Govindarajan, U., Ramachandaramurthy, V.K., *et al.*: 'Multiple criteria decision making (MCDM) based economic analysis of solar PV system with respect to performance investigation for Indian market', *Sustainability*, 2017, **9**, (5), pp. 820–839

[3] Mosa, M., Shadmand, M.B., Balog, R.S., *et al.*: 'Efficient maximum power point tracking using model predictive control for photovoltaic systems under dynamic weather condition', *IET Renew. Power Gener.*, 2017, **11**, (11), pp. 1401–1409

[4] Nammalvar, P., Ramkumar, S., Umadevi, R.: 'Cost effective solitary stage single phase inverter for solar PV integration in to grid', *Int. J. Renew. Energy Res.*, 2018, **8**, (3), pp. 1309–1317

[5] Sen, T., Pragallapati, N., Agarwal, V., *et al.*: 'Global maximum power point tracking of PV arrays under partial shading conditions using a modified particle velocity-based PSO technique', *IET Renew. Power Gener.*, 2018, **12**, (5), pp. 555–564

[6] Metry, M., Shadmand, M.B., Balog, R.S., *et al.*: 'High efficiency MPPT by model predictive control considering load disturbances for photovoltaic applications under dynamic weather condition'. IECON 2015 – 41st Annual Conf. of the IEEE Industrial Electronics Society, Yokohama, 2015, pp. 4092–4095

[7] Qin, L., Xie, S., Hu, M., *et al.*: 'Stable operating area of photovoltaic cells feeding DC–DC converter in output voltage regulation mode', *IET Renew. Power Gener.*, 2015, **9**, (8), pp. 970–981

[8] Liu, J., Li, J., Wu, J., *et al.*: 'Global MPPT algorithm with coordinated control of PSO and INC for rooftop PV array', *J. Eng.*, 2017, **13**, pp. 778–782

[9] Pareek, S., Kishnani, M., Gupta, R.: 'Optimal tuning off PID controller using meta heuristic algorithms'. Int. Conf. on Advances in Engineering & Technology Research (ICAETR – 2014), Unnao, 2014, pp. 1–5

[10] Yazdani, M., Jolai, F.: 'Lion optimization algorithm (LOA): a nature-inspired metaheuristic algorithm', *J. Comput. Des. Eng.*, 2016, **3**, (1), pp. 24–36

[11] Sulaiman, M., Salhi, A.: 'A seed-based plant propagation algorithm: the feeding station model', *Sci. World J.*, 2015, **2015**, p. 16

[12] Lian, K.L., Jhang, J.H., Tian, I.S.: 'A maximum power point tracking method based on perturb-and-observe combined with particle swarm optimization', *IEEE J. Photovoltaics*, 2014, **4**, (2), pp. 626–633

[13] Hartmann, L.V., Vitorino, M.A., Correa, M.B.d.R., *et al.*: 'Combining model-based and heuristic techniques for fast tracking the maximum-power point of photovoltaic systems', *IEEE Trans. Power Electron.*, 2013, **28**, (6), pp. 2875–2885

[14] Fang, G.J., Lian, K.L.: 'A maximum power point tracking method based on multiple perturb-and-observe method for overcoming solar partial shaded problems'. 6th Int. Conf. on Clean Electrical Power (ICCEP), Santa Margherita Ligure, 2017, pp. 68–73

[15] Akyol, S., Alatas, B.: 'Plant intelligence based meta-heuristic optimization algorithms', *Artif. Intell. Rev.*, 2017, **47**, (4), pp. 417–462

[16] de Oliveira, F.M., Oliveira da Silva, S.A., Durand, F.R., *et al.*: 'Grid-tied photovoltaic system based on PSO MPPT technique with active power line conditioning', *IET Power Electron.*, 2016, **9**, (6), pp. 1180–1191

[17] Nammalvar, P., Ramkumar, S.: 'Parameter improved particle swarm optimization based direct-current vector control strategy for solar PV system', *Adv. Electr. Comput. Eng.*, 2018, **18**, (1), pp. 105–112

[18] Wang, X., Harnefors, L., Blaabjerg, F.: 'Unified impedance model of grid-connected voltage-source converters', *IEEE Trans. Power Electron.*, 2018, **33**, (2), pp. 1775–1787

[19] Eghtedarpour, N., Farjah, E.: 'Control strategy for distributed integration of photovoltaic and energy storage systems in DC micro-grids', *Renew. Energy*, 2012, **45**, pp. 96–110
[20] Nagashima, H., Hikosaka, K.: 'Plants in a crowded stand regulate their height growth so as to maintain similar heights to neighbours even when they have potential advantages in height growth', *Ann. Bot.*, 2011, **108**, (1), pp. 207–214
[21] Givnish, T.J.: 'On the adaptive significance of leaf height in forest herbs', *Am. Nat.*, 1982, **120**, pp. 353–381
[22] Anzalchi, A., Sarwat, A.: 'Artificial neural network based duty cycle estimation for maximum power point tracking in photovoltaic systems'. SoutheastCon 2015, Fort Lauderdale, FL, 2015, pp. 1–5
[23] Li, S., Xu, L., Haskew, T.A.: 'Control of VSC-based STATCOM using conventional and direct-current vector control strategies', *Int. J. Electr. Power Energy Syst.*, 2013, **45**, (1), pp. 175–186
[24] Cai, H., Xiang, J., Wei, W.: 'Modelling, analysis and control design of a two-stage photovoltaic generation system', *IET Renew. Power Gener.*, 2016, **10**, (8), pp. 1195–1203